

## MAGNETIC PROPERTIES OF N87 MnZn (EPCOS TYPE) FERRITE

Veronica PALTANEA<sup>1</sup>, Gheorghe PALTANEA<sup>2</sup>, Horia GAVRILĂ<sup>3</sup>,  
Gelu IONESCU<sup>4</sup>

*The energy losses and the permeability dependences of MnZn ferrite ring cores, industrial type N87 EPCOS (Siemens), has been studied at 20 mT at room temperature, 23°C. The investigation has been performed by a fluxmetric method from direct current (DC) to 3 MHz. The behavior of the losses and permeability are presented by the identification of the separate rolls of domain wall (dw) and rotational process at 20 mT. Eddy current mechanisms are not involved in this type of magnetization process, because those mechanisms can be appreciated, in standard materials and cores, only on approaching and overcoming the MHz range.*

**Keywords:** soft ferrites, power transformers, chokes, magnetic losses, temperature behavior

### 1. Introduction

Ferrites are dark grey or black ceramic materials. They are very hard, brittle and chemically inert. Most modern magnetically soft ferrites have a cubic (spinel) structure. The general composition of such ferrites is  $(\underline{M})_m-(\text{Fe}_2\text{O}_3)_n$  where  $\underline{M}$  represents one or several of the divalent transition metals such as manganese (Mn), zinc (Zn), nickel (Ni), cobalt (Co), copper (Cu), iron (Fe) or magnesium (Mg). The most popular combinations are manganese and zinc (MnZn) or nickel and zinc (NiZn). These compounds exhibit good magnetic properties below the Curie temperature ( $T_C$ ) and have a rather high intrinsic electric resistivity. These materials can be used up to very high frequencies without laminating, as is the normal requirement for magnetic metals to reduce the eddy current losses. NiZn ferrites have a very high resistivity and are most suitable for frequencies over 1 MHz, while MnZn ferrites exhibit higher permeability and saturation induction levels and are suitable up to 3 MHz. For some special applications, single crystal ferrites can be produced, but the most types of ferrites are manufactured as polycrystalline ceramics.

---

<sup>1</sup> Assist., Dept. of Electrical Engineering, University POLITEHNICA of Bucharest, Romania

<sup>2</sup> Assist., Dept. of Electrical Engineering, University POLITEHNICA of Bucharest, Romania,  
e-mail: gheorghe.paltanea@upb.ro

<sup>3</sup> Prof., Dept. of Electrical Engineering, University POLITEHNICA of Bucharest, Romania

<sup>4</sup> Assoc. Prof., Dept. of Electrical Engineering, University POLITEHNICA of Bucharest, Romania

Soft ferrite cores are used wherever effective coupling between an electric current and a magnetic flux is required. They form an essential part of inductors and transformers used in today's main application areas: telecommunications, power conversion, interference suppression. Reduction in size and weight of power supplies can be achieved by using switched mode or resonant concepts at increasing frequencies, which may even exceed 1 MHz nowadays. For magnetic components this requires new ferrite grades with increasingly severe demands on low magnetic saturation and eddy current losses. A well-balanced series of MnZn and NiZn power ferrites has been developed for frequencies ranging from 10 kHz to 10 MHz. These materials are applied in highly efficient core assemblies with specially designed core shapes and windings. The industrial type ferrite N87 has very soft behavior and near-insulating character, which makes it ideal for uses in such range of frequencies in the design of power transformers and chokes [1].

In the case of N87 ferrite is defined the temperature  $T_0$ , at which the temperature of the first-order anisotropy constant  $K_1$  is zero. In practical applications of MnZn N87 ferrites, such as transformers,  $T_0$  is controlled to fit the operating temperature, between 80° C and 100° C, by changing the composition of MnZnFeO. As a result, power losses are minimal at that temperature,  $T_m$ . However, in the range between the room temperature and 100° C, the losses in the MnZn ferrites vary significantly. Nevertheless, for use over a wide temperature range, it is convenient to make the temperature dependence of losses smaller [2].

In this paper we present a combined analysis of losses and magnetic permeability, which can be done by using the losses separation concept under very general terms, independent of the dissipation mechanism. It is demonstrated in [3, 4] that the classical energy losses (classical eddy currents losses) contribute to the total energy losses by little to negligible extends and the dominant dissipation mechanism in these ferrites samples is not related to eddy currents.

In order to obtain a complete characterization of the N87 MnZn ferrite we have made an investigation in Rayleigh's domain at the frequency equal to 5 kHz, at room temperature. The analysis of the behavior in Rayleigh's range can provide us the meaning to a direct relationship between energy losses and complex permeability.

## 2. Experimental method

The sintered ferrite ring sample of MnZn (N87) was characterized between 0 and 3 MHz using a fluxmetric method, which is based on a purpose built laboratory hysteresisgraph wattmeter. The experimental setup contains an arbitrary function generator, a power amplifier, a low noise signal amplifier and a four channel oscilloscope.

The sample had an outside diameter of 10 mm and an inside diameter of 6 mm with a thickness of 1.2 mm. Other physical properties are: density  $\rho = 4850 \text{ kg/m}^3$ , average particle size  $\langle s \rangle = 16 \text{ }\mu\text{m}$ , electrical conductivity  $\sigma = 230 \text{ S/m}$  and saturation polarization  $J_s = 0.47 \text{ T}$ .

### 3. Initial magnetization curve and Rayleigh parameters

In the Rayleigh's range the hysteresis cycle has an elliptical shape and it is described by:

$$J = aH + bH^2 \quad (1)$$

The determination of the Rayleigh's parameters  $a$  and  $b$  permits to separate the reversible and irreversible parts, at a given magnetic polarization  $J_p$ , the latter being exclusively due to the domain wall processes. A measurement at 5000 Hz was performed in order to obtain the initial magnetization curve (Fig. 1).

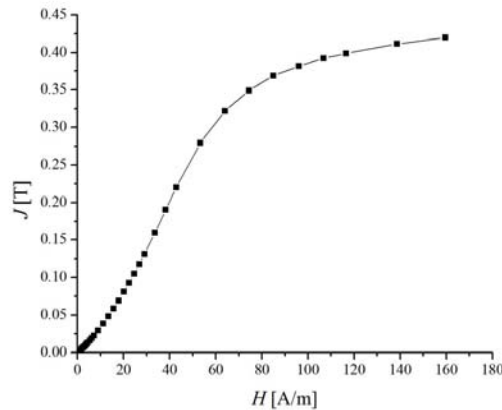


Fig. 1. Initial magnetization curve of sintered MnZn ferrite at room temperature.

In (1)  $a$  is correlated with the reversible magnetization process and is proportional to the initial magnetic susceptibility [5] and  $b$  characterizes the irreversible processes, which are due to the existence of pinning sites in the N87 magnetic material [6]. To determine the values of  $a$  and  $b$  parameters we made a representation of  $J/H(H)$ , which was extrapolated to zero in order to obtain the value of  $a$ , and for  $b$  value was calculated the slope of this figure (Fig. 2).

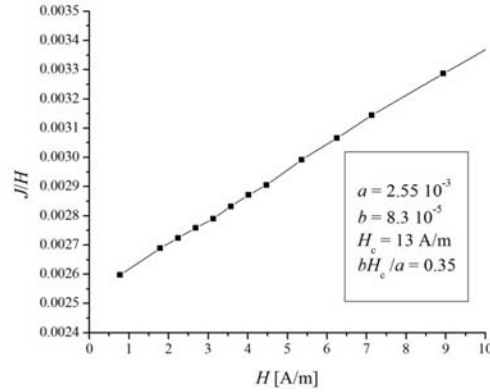


Fig. 2. Determination of Rayleigh's parameters:  $a = 2.55 \cdot 10^{-3}$ ,  $b = 8.3 \cdot 10^{-5}$  and coercive field value  $H_c = 13$  A/m.

In accordance with those values one can assume that in case of the N87 MnZn ferrite the predominant magnetization processes are of the reversible types.

#### 4. Magnetic losses and permeability analysis in N87 ferrite

The evaluation of a magnetic material by producers and users is based on the knowledge of the energy losses parameters.

The use of this soft magnetic material in the medium-to-high frequency range raises problems like energy dissipation and heating in the electronic devices, which call for understanding and prediction of magnetic losses. The energy losses phenomena in N87 MnZn ferrite can be related with three dissipation mechanisms: eddy currents, spin damping and resonance effects, this making the concept of the statistical losses separation theory to be generally assumed.

The energy losses separation was made firstly by accurately extrapolating the experimental  $W(f)$  values to  $f = 0$ , in order to determine the hysteresis energy losses  $W_h$ . Then the classical component  $W_{cl}(f)$  is calculated. Sintered ferrites are actually aggregates of semiconducting grains separated by near-insulating layers. The calculation of  $W_{cl}$  for such heterogeneous structures requires a suitable modeling. The sample can be described as an ordered assembly of identical cubic grains of side  $\langle s \rangle$ , equal to the directly observed average grain size. Each elementary cell has resistivity  $\rho_g$ , boundary layer of thickness  $d_i$ , electrical resistivity  $\rho_i$ , and relative permittivity  $\epsilon_r$ . Each cell can be identified with an equivalent RC circuit and the sample impedance versus frequency was determined [7, 8]. The input data used in calculation of the sample impedance are:  $\rho_g = 4.347 \times 10^{-3} \Omega\text{m}$ ,  $d_i = 0.65 \text{ nm}$ ,  $\rho_i = 0.2 \times 10^6 \Omega\text{m}$ ,  $\epsilon_r = 12$ . Two electromagnetic

problems are now solved. Firstly, a known magnetic flux is imposed through the section and eddy currents and losses are consequently determined. In the second problem a known current is forced to flow through the ferrite section, in order to evaluate the per unit length impedance [8].

The contribution of  $W_{cl}(f)$  to the total energy losses can be appreciated, in all investigated materials and for all sample sizes, only in the MHz range (Fig 3). The main problem in the analysis of energy losses in ferrites is then to identify and possibly predict the component  $W_{exc} = W - W_h - W_{cl}$ , by far the largest contribution to  $W$  at the frequencies of practical interest.

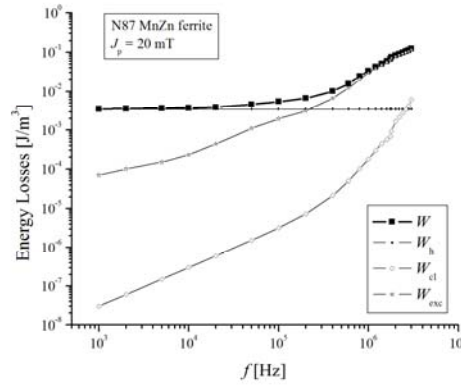


Fig. 3. The experimental energy losses in a MnZn ferrite ring decomposed into hysteresis  $W_h = 3.47 \times 10^{-6} \text{ J/m}^3$ , classical  $W_{cl}$  (obtained through numerical simulation of two electromagnetic problems) and  $W_{exc}$  at peak polarization  $J_p = 20 \text{ mT}$ .

The main dissipation mechanisms in MnZn ferrites are related to the damped motion of the domain walls, which is described by:

$$2J_s(H_a - H_c) = \beta \frac{\partial x}{\partial t} \quad (2)$$

where  $H_a$  is the applied magnetic field,  $\beta$  the damping coefficient and  $\frac{\partial x}{\partial t}$  is the velocity of the moving domain wall. The damping parameter  $\beta$  has two contributions:  $\beta_{sd}$  – due to the viscous precession of the magnetic spins inside the moving domain wall and  $\beta_{eddy}$  – due to eddy currents, which surround the moving domain walls. It was demonstrated, that in ferrites  $\beta_{sd} \gg \beta_{eddy}$ , thus any dynamic contribution to the energy losses directly deriving from the domain wall processes is associated with spin damping [7, 8, 9].

These two parameters are calculated with the following formulas and in the case of N87 MnZn ferrite have the values:

$$\beta_{eddy} = 4\sigma_g G J_s^2 \langle s \rangle = 44.09 \times 10^{-5}, \quad (3)$$

$$\beta_{sd} = \frac{2J_s \alpha_{LL}}{\mu_0 \gamma \delta_w} = 0.209, \quad (4)$$

where:  $\sigma_g$  – the conductivity of the grain,  $G = 0.1356$  – is a constant [10],  $\alpha_{LL} = 0.04$  – Landau-Lifshitz damping constant,  $\mu_0$  – vacuum magnetic permeability,  $\gamma = 1.760 \times 10^{11}$  1/(sT) – electron gyromagnetic ratio,  $\delta_w = \pi \sqrt{\frac{A}{K}} = 0.81 \mu\text{m}$  – domain wall thickness, where:  $A = 2 \times 10^{-12}$  J/m – the macroscopic exchange constant,  $K = 30 \text{ J/m}^3$  – first anisotropy constant.

The expression for excess losses through eddy currents  $W_{exc,eddy}$  can be written taking into the account the damping coefficient  $\beta_{eddy}$  as following [11]:

$$W_{exc,eddy}(J_p, f) = 4 \left[ \beta_{eddy} \left( W_h(J_p)^n \left\langle s \right\rangle \left( \frac{J_p}{J_s} \right) f \right) \right]^{\frac{1}{n+1}} \quad (5)$$

where  $J_p$  is the peak polarization,  $f$  is the working frequency and  $n = 0.5$  is a parameter related to distribution function for the internal coercive fields.

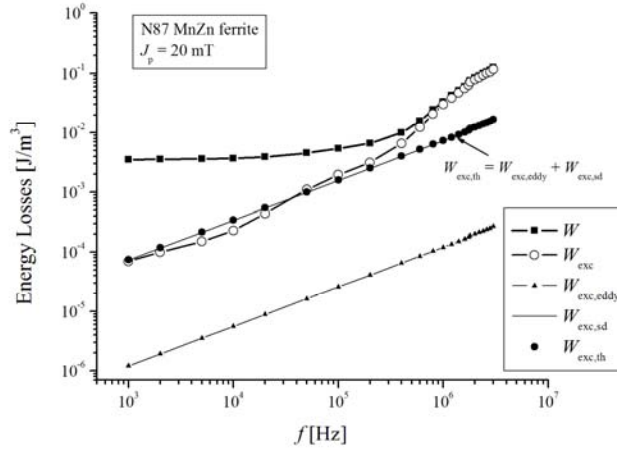


Fig. 4. Theoretical prediction of the two excess energy losses components ( $W_{exc,eddy}$ ,  $W_{exc,sd}$ ) and comparison with the experimental one ( $W_{exc}$ ).

A practical formula for predicting the excess losses through spin damping  $W_{exc,sd}$ , by taking into account the fact that  $W_h$  is associated with the irreversible domain wall processes only, can be now obtained [12]:

$$W_{exc,sd}(J_p, f) = 4 \left[ \beta_{sd} \left( W_h(J_p)^n \left\langle s \right\rangle k_{irr} \left( \frac{J_p}{J_s} \right) f \right) \right]^{\frac{1}{n+1}} \quad (6)$$

where  $k_{irr} = J_{p,irr}/J_p$  is the irreversibly accomplished fraction of the magnetization reversal. This quantity was directly obtained from the experimental initial magnetization curve (see Rayleigh constants). For 20 mT it was obtained  $k_{irr} = 0.09$ . Figure 4 shows that the high frequency part of  $W$  cannot be predicted neither by the domain wall term  $W_{exc,sd}$  nor by the classical eddy-current distribution  $W_{cl}$ . It is known that, under the action of the exciting ac field and the resisting torque provided by the effective anisotropy field, the spins in the bulk are bound to process and release energy to the lattice through the same mechanism involved with the frictional response of the domain walls. The domain wall dynamics is associated with pure relaxation and resonant phenomena are expected to occur with rotations [13]. As presented in [14] soft ferrites are very low anisotropy materials with a large distribution of the anisotropy fields, which have different values from grain to grain, and different resonance frequencies.

The complex relative permeability variation  $\mu = \mu' - j\mu''$  for MnZn N87 sintered ferrite can be found in Fig. 5. It can be seen that for frequencies up to 100 kHz, the real part of complex permeability,  $\mu'$ , is about 2444. As the frequency increases, each measured spectrum remains level at first and then rises to a certain peak before falling rapidly to relatively low values. After 100 kHz the imaginary component,  $\mu''$ , rises to a pronounced peak as  $\mu'$  falls. The relaxation frequency, at which  $\mu''$  has a maximum value, is about  $f_1 = 1.2$  MHz.

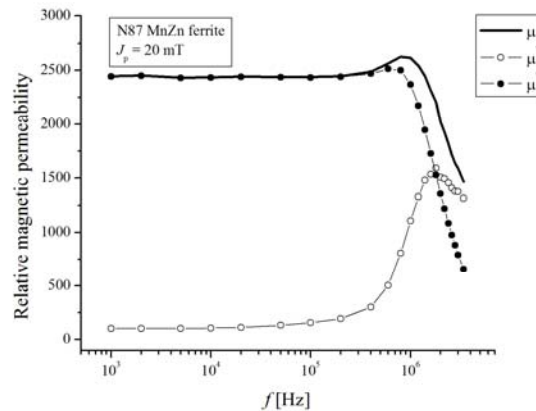


Fig. 5. Experimental values of the complex relative magnetic permeability versus frequency.

One considers in this article, that the complex distribution of the internal fields, to which the resonance frequencies are directly related, can be compiled into a suitable distribution density for the anisotropy field  $H_k$ . For that we consider a Maxwell distribution, which describes the anisotropy fields:

$$f(H_k) = \frac{1}{H_0^3} \sqrt{\frac{2}{\pi}} H_k^2 e^{\left(\frac{-H_k^2}{2H_0^2}\right)} \quad (7)$$

with  $H_0 = 68$  A/m and  $\langle H_k \rangle = 110$  A/m (average resonance frequency  $f_r = \frac{\gamma}{2\pi} \mu_0 \langle H_k \rangle = 3.87$  MHz).

Under small oscillation approximation, the rotational process inside a generic domain, are described by a linear Landau-Lifshitz-Gilbert (LLG) equation. The real  $\chi'_{rot}$  and imaginary  $\chi''_{rot}$  susceptibility values are obtained for any  $H_k$  value as solution of the LLG equation [9, 15, 16]:

$$\chi'_{rot}(f) = \frac{f_j f_H [f_H^2 - f^2(1 - \alpha_{LL}^2)]}{[f_H^2 - f^2(1 + \alpha_{LL}^2)]^2 + 4\alpha_{LL}^2 f_H^2 f^2}, \quad (8)$$

$$\chi''_{rot}(f) = \frac{f_j f \alpha_{LL} [f_H^2 + f^2(1 + \alpha_{LL}^2)]}{[f_H^2 - f^2(1 + \alpha_{LL}^2)]^2 + 4\alpha_{LL}^2 f_H^2 f^2}, \quad (9)$$

where:  $f_j = \gamma J_s / (2\pi)$  and  $f_H = \gamma \mu_0 H_k / (2\pi)$ .

The relative rotational permeabilities are consequently obtained as:

$$\mu'_{rot}(f) = 1 + \langle \chi'_{rot}(f) \rangle, \quad (10)$$

$$\mu''_{rot}(f) = \langle \chi''_{rot}(f) \rangle, \quad (11)$$

with the brackets implying double averaging (i.e.

$\langle x(f) \rangle = \frac{2}{3} \int_0^\infty x(H_k, f) f(H_k) dH_k$ ) over the Maxwell distribution of  $H_k$ ,  $f(H_k)$ , and

an assumed isotropic distribution of the effective easy axes in the material.

Taking into account that the domain wall displacements and rotational processes are independent, the total energy losses can be written as  $W(J_p, f) = W_{dw}(J_p, f) + W_{rot}(J_p, f)$ , where the energy losses by domain wall displacements are due to [9]:

$$W_{dw}(J_p, f) = W_h(J_p) + W_{exc, sd}(J_p, f). \quad (12)$$



According to [12] in the case of low values for magnetic polarization  $J_p = 20$  mT one can obtain an ellipsoidal hysteresis loop shape and for the imaginary component  $\mu''_{dw}(f)$  can be generated the following expression:

$$\mu''_{dw}(f) = \frac{W_{dw}(J_p, f)}{\pi H_p^2(f)} \quad (13)$$

where  $H_p(f)$  is the experimental peak field value.

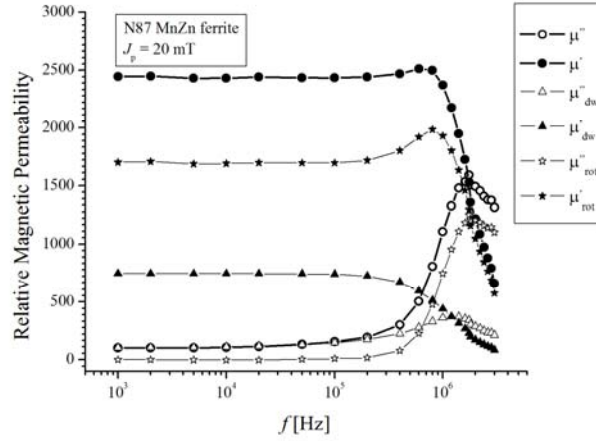


Fig. 6. Real and imaginary relative magnetic permeability components versus frequency at peak polarization  $J_p = 20$  mT (circle: experimentally data obtained).

The dependence  $\mu''_{dw}(f)$  (Fig. 6) can be approximated by a relaxation equation [10]:

$$\mu''_{dw}(f) = \frac{\mu_{dw}(0) \frac{f}{f_1}}{1 + \left(\frac{f}{f_1}\right)^2} \quad (14)$$

where  $f_1 = 1.2$  MHz is the relaxation frequency and  $\mu_{dw}(0)$  is the DC domain wall permeability. Since  $\mu_{dw}(0) = 2\mu''_{dw}(f_1)$ , the real permeability  $\mu'_{dw}(f)$  is calculated as:

$$\mu'_{dw}(f) = \frac{2\mu_{dw}^2(f_1)}{1 + \left(\frac{f}{f_1}\right)^2} \quad (15)$$

Combining the previously determined relative rotational permeabilities and relative domain wall permeabilities as follows:

$$\mu'_{th}(f) = \mu'_{dw}(f) + \mu'_{rot}(f), \quad (16)$$

$$\mu''_{th}(f) = \mu''_{dw}(f) + \mu''_{rot}(f), \quad (17)$$

one can obtain the real and imaginary values of total relative magnetic permeability (Fig. 7).

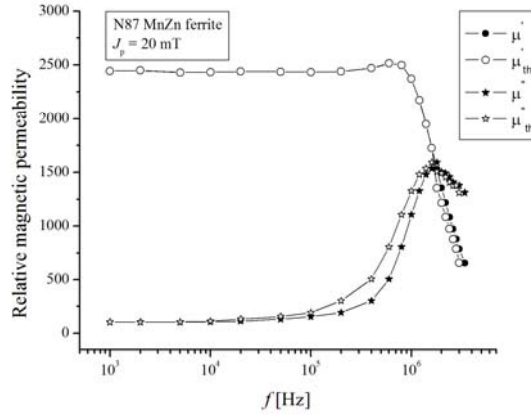


Fig. 7. Comparison between theoretical and experimental complex relative magnetic permeability versus frequency.

In order to obtain the theoretical expression of total energy losses

$$W_{th}(J_p, f) = W_{dw}(J_p, f) + W_{rot}(J_p, f) \quad (18)$$

the energy loss, generated by the rotational processes at a given  $J_p$ , can be written as [12]:

$$W_{rot}(J_p, f) = \frac{\pi J_p^2 \mu''_{rot}(f)}{\mu'_{th} + \mu''_{th}} \quad (19)$$

In Fig.8 it is presented a comparison between the experimental values of the total energy losses and the values obtain by (18), which provide a good description of the experimental loss behavior.

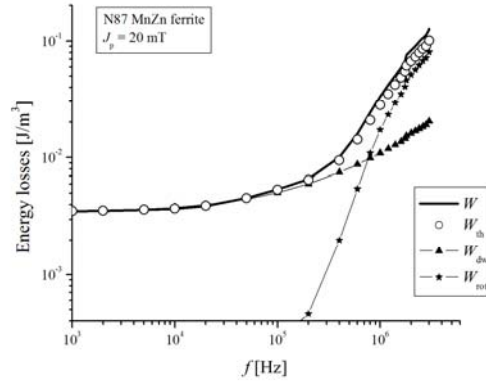


Fig. 8. Comparison between theoretical and experimental total energy losses versus frequency.

## 5. Conclusions

Using the physical concept of loss separation the wide band magnetic properties of N87 soft ferrite is interpreted at peak polarization of 20 mT. In this article the behavior of domain wall and rotational magnetization processes are analyzed under increasing magnetizing frequencies. Different components of the energy loss and their variation versus frequency are identified and calculated starting from the standard equation for the damped motion of the domain wall in the background, offered by the statistical theory of losses. The prediction of the energy loss is based on the linear approximation of the Landau – Lifshitz – Gilbert equation and its application under distributed anisotropy fields.

In the N87 MnZn ferrite the principle magnetization process, on approaching the MHz range, is related to the domain wall movement and for high frequency the magnetization rotations are the main magnetization process.

## REFERENCES

- [1] \*\*\* EPCOS Product Catalog, 2012.
- [2] J.A. Fujita, S. Gotoh, "Temperature dependence of core loss in Co-substituted MnZn ferrites", J. Appl. Phys., **93**, 2003, pp. 7477-7479.
- [3] O. Bottauscio, M. Chiampi, A. Manzin, "Influence of constitutive parameters in soft ferrites: A modeling analysis by homogenization technique", J. Magn. Magn. Matter., **304**, 2006, pp. e746.
- [4] O. Bottauscio, V. Chiado Piat, M. Chiampi, M. Codegone, A. Manzin, "A mathematical approach to loss estimation in non-homogeneous magnetic materials", J. Magn. Magn. Matter., Vol. 290, 2005, pp. 1450.
- [5] H. Gavrilă, et al., Magnetism Tehnic și Aplicat (Technical and Applied Magnetism), Ed. Academiei Române, București, 2000.

- [6] *V. H. Calle, F. Cuéllar, C. Calle, O. Marín, J. Roa-Rojas, D. Arias, O. Guzmán, J. Prado, M. E. Gómez, U.G. Volkmann, P. Prieto, A. Mendoza*, “Pinning energy of domain walls in MnZn ferrite films”, *Physica Status Solidi (C)*, **4**, Issue 11, November 2007, pp. 4197–4202.
- [7] *D. Stoppels*, “Developments in soft magnetic power ferrites”, *J. Magn. Magn. Mater.*, **160**, 1996, pp. 323–328.
- [8] *O. Bottauscio, M. Chiampi, A. Manzin*, “Influence of constitutive parameters in soft ferrites: A modeling analysis by homogenization technique”, *J. Magn. Magn. Mater.*, **306**, 2006, e746–748.
- [9] *F. Fiorillo, C. Beatrice*, “Energy losses in soft magnets from DC to Radiofrequencies: theory and experiment”, *J. Supercond. Nov. Magn.*, **24**, 2011, pp. 559–566.
- [10] *G. Bertotti*, *Hysteresis in Magnetism*, Academic Press, San Diego, 1998.
- [11] *G. Bertotti*, “Direct relation between hysteresis and dynamic losses in soft magnetic materials”, *J. Phys.*, 46-C6, 389, 1985.
- [12] *F. Fiorillo, E. Ferrara, M. Coisson, C. Beatrice, N. Banu*, “Magnetic properties of soft ferrites and amorphous ribbons up to radiofrequencies”, *J. Magn. Magn. Mater.*, **322**, 2010, pp. 1497–1504.
- [13] *E.G. Visser*, “Effect of uniaxial tensile stress on the permeability of monocrystalline MnZnFe ferrite”, *J. Appl. Phys.*, **55**, 1984, p. 2251–2253.
- [14] *P. Gelin, P. Queffelec*, “Effect of domain and grain shapes on the dynamical behavior of polycrystalline ferrites: Application to the initial permeability”, *J. Appl. Phys.*, **98**, 2005.
- [15] *G. Bertotti, I.D. Mayergoyz, C. Serpico*, “Identification of the damping coefficient in Landau – Lifshitz equation”, *Physica B*, **306**, 2001, pp. 102–105.
- [16] *S. Bartels, J. Ko, A. Prohl*, “Numerical analysis of an explicit approximation scheme for the Landau-Lifshitz-Gilbert equation”, *Math. Comp.*, **77**, 2008, pp. 773–788.